# Models of Nitric Oxide Synthase: Iron(III) Porphyrin-Catalyzed Oxidation of Fluorenone Oxime to Nitric Oxide and Fluorenone

**Charles C.-Y. Wang, Douglas M. Ho, and John T. Groves***

*Contribution from the Department of Chemistry, Princeton University, Princeton, New Jersey 08544*

*Received July 8, 1999*

**Abstract:** Nitric oxide synthase (NOS) is a heme-containing monoxygenase that catalyzes the oxidation of L-arginine to L-citrulline and NO in two steps. In the second step of the NOS reaction, citrulline and NO are generated from the heme-catalyzed 3-electron oxidation of L-*N*-hydroxyarginine. To model this unusual reaction, iron porphyrin-catalyzed oxygenations of oximes with $O_2$ were investigated. The oxidation of fluorenone oxime and a stoichiometric amount of hydroxoiron(III) porphyrin (Fe(OH)P, P = TMP and TPFPP) with $O_2$ in benzene generated Fe(NO)P, fluorenone, and *O*-(9-nitro-9-fluorenyl)fluorenone oxime. The X-ray crystal structure of the oxime ether product suggests that it originated from the dimerization of the fluorenyl iminoxy radicals. Detailed analysis of this reaction showed that the oxime reacted first with Fe(OH)P to generate a 5-coordinate, high-spin oximatoiron(III) porphyrin species [Fe(oximate)P]. The X-ray crystal structure of oximatoiron(III) tetrakis(2,6-dichlorophenyl)porphyrin [Fe(oximate)TDCPP] showed that the oximate ligand was monodentate, O-bound to Fe(III)P. The aerobic oxidation of Fe(oximate)P followed the characteristic kinetics of a metalloporphyrin-catalyzed radical-type autoxidation. $O_2$ surrogates, the $\pi$-acids NO and CO, induced the homolysis of Fe(oximate)P to generate Fe(NO)P or Fe(CO)P and the iminoxy radical, implicating a similar reaction mode for $O_2$ with Fe(oximate)P. Fe(oximate)TMP reacted with $^{18}O_2$ to generate predominantly $^{18}O$-labeled fluorenone (75% yield), while the reaction conducted under $^{16}O_2$ and $H_2{}^{18}O$ generated only $^{16}O$-labeled fluorenone. This reaction is proposed to proceed via an Fe−O bond homolysis of Fe(oximate)TMP followed by $O_2$ insertion to generate 9-nitroso-9-fluorenylperoxyFe(III)TMP, which decomposes via an O−O bond homolysis to generate NO, fluorenone, and oxoFe(IV)P. The implications of this system for the NOS reaction mechanism are discussed.

## Introduction

Nitric oxide (NO) is a ubiquitous biomessenger[1,2] with a variety of functions including blood vessel dilation,[3] neuronal signal transmission,[4] cytotoxicity against pathogens and tumors,[5] and cellular respiration activity.[6] The over- or underproduction of NO has also been implicated in a number of pathological symptoms such as endotoxic shock,[7] diabetes,[8] allograft rejection,[9] and myocardial ischimia/reperfusion injury.[10]

NO is generated by the oxidation of L-arginine by $O_2$ mediated by nitric oxide synthase (NOS; EC 1.14.13.39). Four isoforms of NOS have been discovered: a constitutive, calmodulin-dependent neuronal NOS (nNOS), endothelial NOS (eNOS), mitochondrial NOS (mtNOS),[11,12] and the calmodulin-independent, cytokine-inducible NOS (iNOS). All NOS isoforms contain the cysteinyl thiolate-ligated Fe(III) heme feature[13−16] and extensive homology of their reductase domains to cytochrome P450 reductase.[17,18]

**Scheme 1**

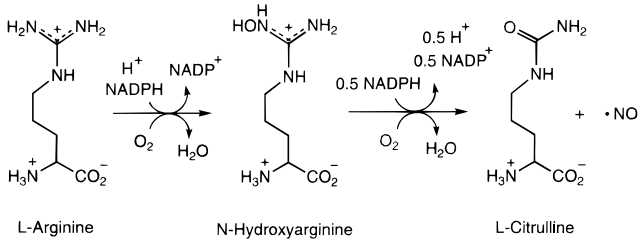


NOS catalyzes the 5-electron oxidation of arginine to citrulline and NO in two steps[19] (Scheme 1). In the first step, two NADPH-derived reducing equivalents and $O_2$ afford *N*-hydroxyarginine (NHA). The redox stoichiometry is that of a typical P450-like hydroxylation. The second step of the NOS reaction involves a 3-electron oxidation of *N*-hydroxyarginine

* To whom correspondence should be addressed

(1) Dangl, J. *Nature* **1998**, *394*, 525.
(2) Muller, U. *Prog. Neurobiol.* **1997**, *51*, 363.
(3) Hansen, M. B.; Dresner, L. S.; Wait, R. B. *Physicol. Res.* **1998**, *47*, 307.
(4) Agnihotri, N.; Lopez-Garcia, J. C.; Hawkins, R. D.; Arancio, O. *Histol Histopathol* **1998**, *13*, 1155.
(5) Albina, J. E.; Reichner, J. S. *Cancer Metastasis Rev.* **1998**, *17*, 39.
(6) Brown, G. C. *Biochim. Biophys. Acta: Bioenerget.* **1999**, *1411*, 351.
(7) Shah, N. S.; Billiar, T. R. *Environ. Health Perspect.* **1998**, *106*, 1139.
(8) Cosentino, F.; Luscher, T. F. *J. Cardiovasc. Pharmacol.* **1998**, *32*, s54.
(9) Liu, Z. Q.; Wildhirt, S. M.; Weismuller, S.; Schulze, C.; Conrad, N.; Reichart, B. *Atherosclerosis* **1998**, *140*, 1.
(10) Hammerman, C. K. M. *Clin. Perinatol.* **1998**, *25*, 757.
(11) Ghafourifar, P.; Richter, C. *FEBS Lett.* **1997**, *418*, 291.
(12) Tatoyan, A.; Giulivi, C. *J. Biol. Chem.* **1998**, *273*, 11044.
(13) Mcmillan, K.; Bredt, D. S.; Hirsch, D. J.; Snyder, S. H.; Clark, J. E.; Master, B. S. S. *Proc. Natl. Acad. Sci. U.S.A.* **1992**, *84*, 6369.
(14) Klatt, P.; Schmidt, K.; Mayer, B. *Biochem. J.* **1992**, *288*, 15.
(15) Stuehr, D. J.; Ikeda-Saito, M. *J. Biol. Chem.* **1992**, *267*, 20547.
(16) White, K. A.; Marletta, M. A. *Biochemistry* **1992**, *31*, 6627.
(17) Bredt, D. S.; Hwang, P. M.; Glatt, C. E.; Lowenstein, C.; Reed, R. R.; Snyder, S. H. *Nature* **1991**, *351*, 714.
(18) Xie, Q. W.; Cho, H. J.; Calycay, J.; Mumford, R. A.; Swiderek, K. M. *Science* **1992**, *256*, 225.
(19) Hemmens, B.; Mayer, B. In *Nitric Oxide Protocols*; Titheradge, M. A., Ed; Humana: Totowa, NJ , 1998; Vol. 100, p 1.

10.1021/ja992373+ CCC: $18.00 
Published on Web 12/15/1999

to NO and citrulline by $O_2$ with the consumption of only one NADPH-derived reducing equivalent.[20,21] $^{18}O$-labeling experiments have shown that the urea oxygen of citrulline is derived from $O_2$, while the NO product originates exclusively from the *N*-hydroxy group of NHA.[22,23] Nevertheless, the mechanistic details of this unusual second step of the NOS reaction mechanism are still unclear.

A key unanswered question is the order of the redox events involved in the oxidation of NHA. Particularly, it is unclear whether the NOS Fe(III) heme is reduced by NHA or the NADPH-derived reducing equivalent to initiate the second step. Several proposals have been advanced to account for these unusual redox events. They include an oxoFe(IV) porphyrin radical cation active species reminiscent of the cytochrome P450 monooxygenase-type mechanism,[24,25] and versions of a nucleophilic peroxoFe(III)P species analogous to that proposed for the aromatase reaction.[20,26−29]

An understanding of the detailed reaction mechanism of the NOS reaction is not only of intrinsic interest but is also important for the rational design of selective NOS inhibitors.[30,31] Chemical reactions that mimic the important features of the NHA oxidation could be powerful tools for deciphering its mechanism.

We have discovered that the Fe(III)P-catalyzed aerobic oxidation of oximes produces NO and ketones. This reaction was initiated by coordination of the oxime to the Fe(III) porphyrin. Further, reactions conducted under $^{18}O_2$ generated $^{18}O$-labeled product distribution patterns similiar to those of the NOS reaction.

## Results and Discussion

Fluorenone oxime reacted with a stoichiometric amount of hydroxoiron(III) porphyrins (Fe(OH)P, P = TMP and TPFPP) under $O_2$ to generate nitrosyliron(II) porphyrin (Fe(NO)P), fluorenone, and a novel dimer derivative (**1**; see Table 1) of fluorenyl iminoxy radical (Scheme 2). For example, a one-to-one ratio of fluorenone oxime and Fe(OH)TMP in benzene-$d_6$ (0.75 mM) was oxidized with greater than 95% conversion after exposure to 500 psi $O_2$ for 9 h. The $^1H$ NMR spectrum of this reaction mixture showed that the iron porphyrin was converted to Fe(OH)TMP, Fe(NO)TMP, Fe($NO_3$)TMP,[32] and a new 5-coordinate high-spin Fe(III)TMP species, which we tentatively assigned as a nitritoFe(III) complex (Fe(ONO)TMP).[33] The product distribution of the Fe(III)TMP-mediated aerobic oxidation of the oxime was found to be dependent on the $O_2$ pressure. As shown in Table 2, the higher the headspace $O_2$ pressure, the higher the yields of fluorenone, Fe($NO_3$)TMP, and the putative Fe(ONO)TMP. Concomitantly, the yields of the fluorene-based dimer and Fe(NO)TMP decreased as the headspace $O_2$ pressure was raised. Fluorenone was always the major (>80% yield) organic product, and **1** was the only other organic product (<20% yield) of the reaction.

**Table 1.** Summary of X-ray Crystallographic Data of *O*-(9-Nitro-9-fluorenyl)fluorenone Oxime (**1**) and Fe(oximate)TDCPP (**3**)

| | **1** | **3** |
|---|---|---|
| formula | $C_{26}H_{16}N_2O_3$ | $C_{57}H_{28}Cl_8FeN_5O\cdot C_6H_5Cl\cdot 0.5C_7H_{16}$ |
| FW | 404.41 | 1300.94 |
| color/habit | pale yellow/irregular | dark purple/prism |
| cryst system | monoclinic | triclinic |
| space group | $P2_1/n$ | $P\bar{1}$ |
| *a*, Å | 9.8776(6) | 12.5029(2) |
| *b*, Å | 11.9206(6) | 13.0424(4) |
| *c*, Å | 17.4262(12) | 18.9793(5) |
| α, deg | 90.00 | 81.701(1) |
| *β*, deg | 101.550(3) | 88.304(2) |
| *χ*, deg | 90.00 | 84.263(2) |
| *V*, Å$^3$ | 2010.3(2) | 3046.80(13) |
| *Z* | 4 | 2 |
| *T*, °C | 25(2) | 25(2) |
| $\rho_{calcd}$, g cm$^{-3}$ | 1.336 | 1.418 |
| $\mu$(Mo Kα), mm$^{-1}$ | 0.089 | 0.690 |
| 2*θ* range, deg | 4.16−44.96 | 3.58−54.92 |
| total no. of data | 26 402 | 79 647 |
| no. of unique data | 2622 | 13 775 |
| no. of observed data[a] | 1948 | 7272 |
| no. of parameters | 416 | 649 |
| $R^b$ | 0.057 | 0.057 |
| $wR^c$ | 0.141 | 0.14 |

[a] With $I > 2\sigma(I)$. [b] $R = \sum|F_o - F_c|/\sum F_o$. [c] $wR = [\sum w(F_o^2 - F_c^2)^2/\sum w(F_o^2)^2]^{1/2}$.

**Scheme 2**

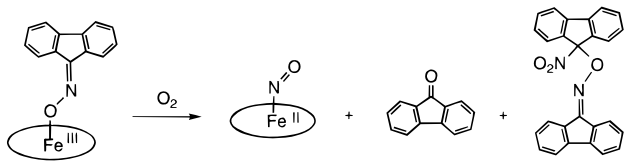


**1**

**Coordination of Fluorenone Oxime to Fe(III)P.** To elucidate the mechanism of this process, we have dissected and characterized the reaction in detail. The reaction of a stoichiometric amount of fluorenone oxime and Fe(OH)P in benzene was found to generate a new 5-coordinate, high-spin Fe(III)P species. The $^1H$ NMR spectrum of this reaction mixture showed that, immediately upon mixing, the resonance signals of Fe(OH)TMP (*δ*80, pyrrole-H; *δ* 11 and 12, *m*-phenyl H) changed

(20) Korth, H. G.; Sustmann, R.; Thater, C.; Butler, A. R.; Ingold, K. U. *J. Biol. Chem.* **1994**, *269*, 17776.
(21) Hevel, J. M.; Marletta, M. A. In *Advances in experimental medicine and biology*; Ayling, J. E., Nair, M. G., Baugh, C. M., Eds; Plenum Press: New York, 1993; Vol. 338, p 285.
(22) Leone, A. M.; Palmer, R. M. J.; Knowles, R. G.; Francis, P. L.; Ashton, D. S.; Moncada, S. *J. Biol. Chem.* **1991**, *266*, 23790.
(23) Kwon, N. Y.; Nathan, C. F.; Gilker, C.; Griffith, O. W.; Matthews, D. E.; Stuehr, D. J. *J. Biol. Chem.* **1990**, *265*, 13442.
(24) Bec, N.; Gorren, A. C. F.; Voelker, C.; Mayer, B.; Lange, R. *J. Biol. Chem.* **1998**, *273*, 13502.
(25) Klatt, P.; Schmidt, K.; Mayer, B. *J. Biol. Chem.* **1993**, *268*, 14781.
(26) Akhtar, M.; LeeRobichaud, P.; Akhtar, M. E.; Wright, J. N. *J. Steroid Biochem. Mol. Biol.* **1997**, *61*, 127.
(27) Zhang, H. Q.; Dixon, R. P.; Marletta, M. A.; Nikolic, D.; VanBreemen, R.; Silverman, R. B. *J. Am. Chem. Soc.* **1997**, *119*, 10888.
(28) Marletta, M. A. *J. Biol. Chem.* **1993**, *268*, 12231.
(29) Kerwin, J. J. F.; Feldman, P. L.; Lancaster, J. R. *J. Med. Chem.* **1995**, *38*, 4344.
(30) Fukuto, J. M.; Chaughuri, G. *Annu. Rev. Pharmacol. Toxicol.* **1995**, *35*, 165.
(31) Marletta, M. A. *J. Med. Chem.* **1994**, *37*, 1899.
(32) Phililipi, M. A.; Baenziger, N.; Goff, H. M. *Inorg. Chem.* **1981**, *20*, 3934.

(33) (a) A 5-coordinate nitritoFe(III) porphyrin species has never been characterized. Munro and Sheidt have shown that Fe(Tpiv)($NO_2$) is a low-spin, N-bound nitro complex on the basis of EPR evidence. (Munro, O. Q.; Scheidt, W. R. *Inorg. Chem.* **1998**, 37, 2308.) Similar to Fe(Tpiv)($NO_2$), the high-spin Fe(III)TMP species reported here was detected by $^1H$ NMR as the only intermediate in the aerobic oxidation of Fe(NO)TMP to Fe($NO_3$)TMP. (b) The same high-spin Fe(III)TMP species could also be prepared by extensively evacuating the 6-coordinate low-spin Fe(NO)($NO_2$)-TMP complex. Fe(NO)($NO_2$)TMP was prepared from NO and Fe(OH)-TMP in toluene-$d_8$ by modifying a literature method, (Ellison, M. K.; Schulz, C. E.; Scheidt, W. R. *Inorg. Chem.* **1999**, *38*, 100), and it gave $^1H$ NMR ($C_7D_8$, 270 MHz) signals at *δ* 1.75 (s, 12H), 2.0 (s, 12H), 2.5 (s, 12H), and 8.8 (s, 8H, pyrrole-H). (c) An *O*-nitrito analogue Fe(III)(TTP)[ONC($CN)_2$] has been reported to be high-spin. (Bohle, D. S.; Conklin, B. J.; Hung, C.-H. *Inorg. Chem.* **1995**, *34*, 2569.) Accordingly, we tentatively assigned the high-spin Fe(III)TMP species as the O-bound nitritoFe(III)TMP complex (Fe(ONO)TMP).

**Table 2.** Product Distribution of $O_2$-Effected Oxidation of Fe(oximate)TMP[a] at Different $O_2$ Pressures

| $pO_2$[b] (reaction time)[c] | dimer[d] | Fl═O[e] | dimer/Fl═O ratio | Fe(NO)P | Fe(ONO)P | $Fe(NO_3)P$ | Fe(OH)P |
|---|---|---|---|---|---|---|---|
| 14.7 (3 weeks) | 0.10[f] | 0.80 | 0.13 | 0.24 | 0.20 | 0.36 | 0.20 |
| 100 (72 h) | 0.09 | 0.82 | 0.11 | 0.05 | 0.28 | 0.49 | 0.18 |
| 200 (30 h) | 0.08 | 0.84 | 0.10 | 0.04 | 0.32 | 0.48 | 0.16 |
| 500 (6 h) | 0.07 | 0.86 | 0.08 | 0.04 | 0.27 | 0.55 | 0.14 |

[a] A 0.8 mM benzene-$d_6$ solution of Fe(oximate)TMP was used in each experiment, and the products were analyzed with $^1$H NMR spectroscopy. [b] $O_2$ pressures are reported in psi. [c] The time length required for 50% Fe(oximate)TMP to be consumed. [d] Dimer, compound **1**. [e] Fl═O, fluorenone. [f] Yields are expressed in equivalents relative to the Fe(oximate)TMP consumed.

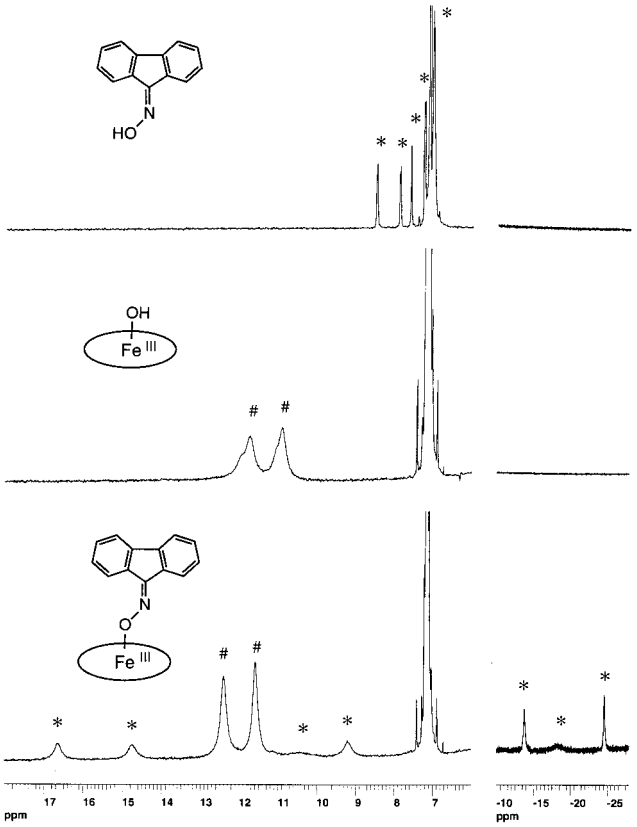


**Figure 1.** $^1$H NMR spectra of the reaction of a one-to-one ratio of fluorenone oxime and Fe(OH)TMP in benzene-$d_6$ at 25 °C. Labels: #, *m*-phenyl protons of the Fe(III)TMP species; *, protons of fluorenone oxime and the oximate ligand.

to those of a new Fe(III)TMP species (**2**; $\delta$ 78, pyrrole-H; $\delta$ 11.7 and 12.5, *m*-phenyl-H) (Figure 1). The pyrrole-H signal of **2** was characteristic of a 5-coordinate, high-spin Fe(III)P species,[34] which indicated that **2** had only one axial ligand (eq 1). Concurrently, the $^1$H NMR resonance signals of fluorenone oxime ($\delta$ 8.5 (d, 1H); 7.9 (d, 1H); 7.3 (m, 2H); 7.0−7.1 (m, 4H)) changed to a group of widely spread, broad signals ($\delta$ 9.2, 10.5, 14.7, 16.6, −20, −25, and −30, with one H at each position).

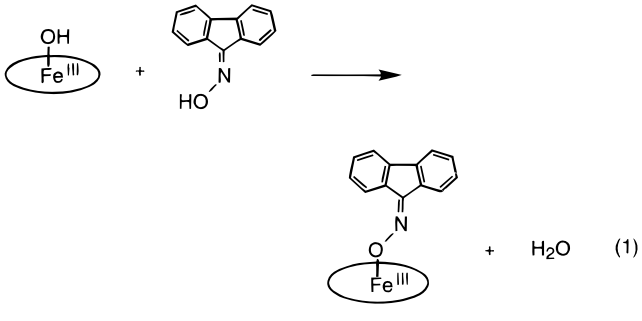


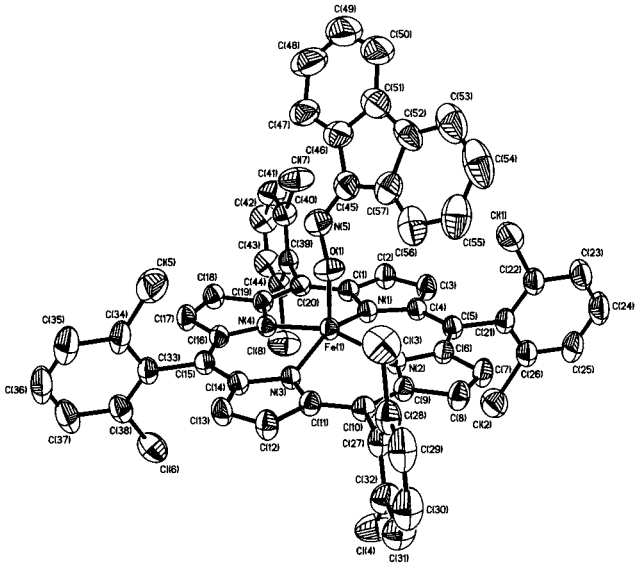

**Figure 2.** Structure of Fe(oximate)TDCPP (**3**) showing 35% probability thermal ellipsoids for all non-hydrogen atoms.

The structure of the oximate-containing Fe(III)P species was determined by an X-ray crystallographic analysis of a single crystal of Fe(oximate)TDCPP (**3**) as shown in Figure 2. Complex **3** contains a single fluorenone oximate ligand oxygen-bound to a 5-coordinate Fe(III) cation. This observed binding mode is rather unusual. More commonly, oximes and oximates bind to metal ions through nitrogen.[35,36] To date, the only iron porphyrin complexes containing oxygen-bound monodentate oximate ligands are complex **3** and Fe[OCN(CN)$_2$]TTP.[37]

There are two notable features in the structure of **3** (Table 3). The first is the nearly equal C−N (1.334 Å) and N−O (1.343 Å) bond distances in the oximate ligand. The C−N bond is slightly (0.04−0.07 Å) longer than C−N double bonds (1.26−1.29 Å) in oximes[38] but is much shorter (0.15−0.19 Å) than C−N single bonds (1.48−1.52 Å) in nonconjugated *C*-nitroso compounds.[39] The N−O bond is 0.04−0.08 Å shorter than N−O single bonds (1.38−1.42 Å) in oximes[38] but is 0.13−0.2 Å longer than N−O double bonds (1.14−1.21 Å) in nonconjugated *C*-nitroso compounds.[39] These observations suggest that the $\pi$

(34) Goff, H. M. In *Physical Bioinorganic Chemistry Series. Iron Porphyrins, Part I*; Levere, A. B. P., Gray, H. B., Eds; Addison-Wesley: Reading, MA, 1983; p 240.
(35) Chakravorty, A. *Coord. Chem. Rev.* **1974**, *13*, 1.
(36) Kukushkin, V. Y.; Tudela, D.; Pombeiro, A. J. L. *Coord. Chem. Rev.* **1996**, *156*, 333.
(37) Bohle, D. S.; Conklin, B. J.; Hung, C.-H. *Inorg. Chem.* **1995**, *34*, 2569.
(38) Ianelli, S.; Nardelli, M.; Belletti, D.; Jamart-Grégoire, B.; Caubère, P. *Acta Crystallogr.* **1992**, *C48*, 1734.
(39) Miao, F.-M.; Chantry, D.; Harper, T.; Hodgkin, D. C. *Acta Crystallogr.* **1982**, *B38*, 3152.

**Table 3.** Selective Bond Lengths (Å) and Angles (deg) of *O*-(9-Nitro-9-fluorenyl)fluorenone Oxime (**1**) and Fe(oximate)TDCPP (**3**)[a]

| bond lengths | | bond angles | |
|---|---|---|---|
| | Compound **1** | | |
| O1*−N1* | 1.442(12) | O1*−C18−N2 | 109.7(3) |
| O1*−C18 | 1.480(9) | O1*−C18−C17A | 125.5(4) |
| O2−N2 | 1.188(3) | O1*−C18−C18A | 97.8(4) |
| O3−N2 | 1.195(3) | O2−N2−O3 | 123.2(3) |
| N1*−C9* | 1.286(12) | O2−N2−C18 | 117.1(3) |
| N2−C18 | 1.569(4) | O3−N2−C18 | 119.7(3) |
| C18−C17A | 1.499(5) | N1*−O1*−C18 | 106.0(8) |
| C18−C18A | 1.507(4) | C9*−N1*−O1* | 109.4(9) |
| | Compound **3** | | |
| Fe1−O1 | 1.836(2) | Fe1−O1−N5 | 126.9(2) |
| Fe1−N1 | 2.060(2) | O1−Fe1−N1 | 105.6(1) |
| Fe1−N2 | 2.073(2) | O1−Fe1−N2 | 99.7(1) |
| Fe1−N3 | 2.056(2) | O1−Fe1−N3 | 99.6(1) |
| Fe1−N4 | 2.058(2) | O1−Fe1−N4 | 105.2(1) |
| O1−N5 | 1.343(3) | O1−N5−C45 | 112.4(3) |
| N5−C45 | 1.334(5) | | |

[a] Numbers in parentheses are estimated standard deviations. Atoms are labeled as indicated in Figures 2 and 3.

system extends over the C−N and N−O bonds but with a greater $\pi$ bond density located on the C−N bond. Similar observations have been reported for the structure of Fe[OCN-$(CN)_2$]TTP; i.e., the corresponding C−N and N−O bond distances are 1.300 and 1.330 Å, respectively.

The other notable feature in **3** is a relatively short Fe−O bond (1.84 Å). Monodentate oxyanion-ligated 5-coordinate Fe(III)P complexes typically exhibit longer Fe−O bonds, e.g., 1.90−2.07 Å. The Fe−O bond (1.945 Å) in Fe[$OCN(CN)_2$]TTP is such an example. The only exceptions have been Fe−O bonds in methoxyFe(III)P (Fe−O bond length, 1.82−1.85 Å)[40−43] and phenoxyFe(III)P complexes (Fe−O bond length, 1.85−1.87 Å).[44,45] It is interesting to note that all of the methoxyFe(III)P complexes contain a planar porphyrin ring with the Fe atom displaced 0.44−0.49 Å from the porphyrin plane. The porphyrin ring in **3** is also planar, and the Fe atom is 0.45 Å out of the porphyrin plane. By contrast, the porphyrin ring in Fe[OCN-$(CN)_2$]TTP is saddle-distorted, and the Fe atom is only 0.36 Å out of the plane defined by the four porphyrin nitrogens.

**Structure of the Organic Dimer 1.** The dimer species **1** was characterized by X-ray crystallography to be *O*-(9-nitro-9-fluorenyl)fluorenone oxime as shown in Figure 3. Species **1** contains two fluorene moieties linked by an oxime ether bridge, and the nitro group is attached to the fluorenyl C-9 atom bonded to the oximyl-O end of the bridge. Only two other compounds with an *O*-(α-nitroalkyl)oxime ether functional group have been structurally characterized.[46,47] Mechanistic studies indicated that both compounds were generated via the dimerization of iminoxy radical species.[48,49] An *O*-(α-nitrosoalkyl)oxime dimer structure

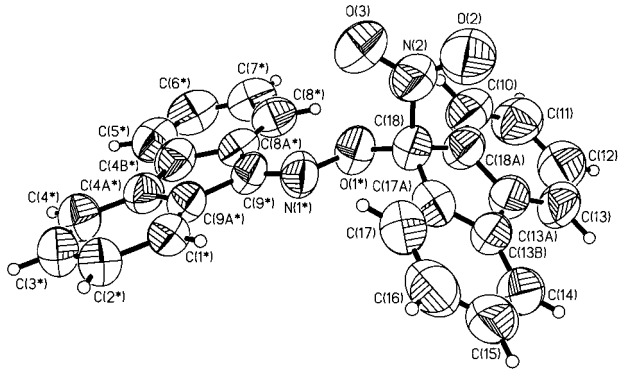


**Figure 3.** Structure of *O*-(9-nitro-9-fluorenyl)fluorenone oxime (**I**) showing 50% probability thermal ellipsoids for all non-hydrogen atoms.

has been crystallographically characterized in the product of metal-mediated, 1-electron oxidation of oximes.[36] For example, *cis*-[$PtCl_4(Me_2C{=}NOH)_2$] spontaneously converted to [Pt(II)-$Cl_2(N(=O)CMe_2ONCMe_2)$] via the Pt(IV)-mediated 1-electron oxidation of the oxime to form the *O*-(α-nitrosoisopropyl)-acetone oxime ligand.[50] The fluorenyl iminoxy radical is known to dimerize rapidly ($k = 2 \times 10^4\ M^{-1}\ s^{-1}$).[51] Thus, we conclude that, during the oxidation of Fe(oximate)P, fluorenyl iminoxy radicals were generated from the Fe−O bond homolysis with subsequent dimerization to form *O*-(9-nitroso-9-fluorenyl)-fluorenone oxime. Further oxidation of the nitroso group of the iminoxy radical dimer by $O_2$ would generate observed *O*-(9-nitro-9-fluorenyl)fluorenone oxime[52] (eq 2).

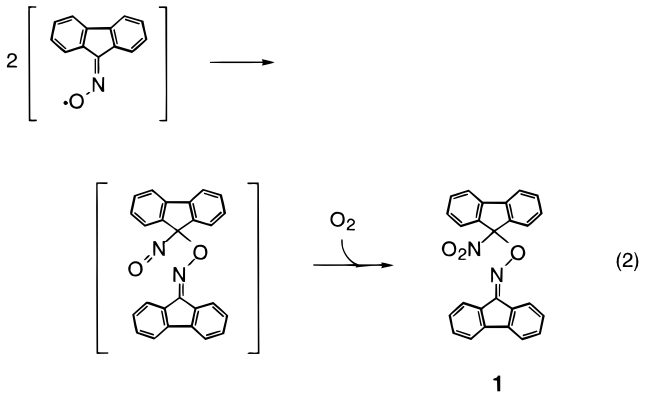


(2)

**1**

**Kinetic Effects of Oxygen Pressure.** The $O_2$-effected oxidation of Fe(III)(oximate)P was found to show the characteristics of a metalloporphyrin-catalyzed radical-type autoxidation.[53] The kinetic profile of the reaction was biphasic with an induction period followed by a fast phase of oxidation. This feature was revealed by observing changes in the $^1$H NMR spectra of benzene-$d_6$ solutions of **2** (0.8 mM) under 500 psi $O_2$. As shown in Figure 4, complex **2** remained intact for 4.5 h until the fast oxidation took place. The fast oxidation completely consumed **2** in a period of another 5 h. Both the induction time and the fast phase oxidation of the reaction could be shortened by increasing the $O_2$ pressure. As the $O_2$ pressure was increased

(40) Hoard, J. L.; Hamor, M. J.; Hamor, T. A.; Caughty, W. S. *J. Am. Chem. Soc.* **1965**, *87*, 2312.
(41) Lecomte, C.; Chadwick, D. L.; Coppens, E. D.; Stevens, E. D. *Inorg. Chem.* **1983**, *22*, 2982.
(42) Hatano, K.; Uno, T. *Bull. Chem. Soc. Jpn.* **1990**, *63*, 1825.
(43) Johnson, M. R.; Seok, W. K.; Ma, W.; Slebodnick, C.; Wilcoxen, K. M.; Ibers, J. A. *J. Org. Chem.* **1996**, *61*, 3298.
(44) Goff, H. M.; Shimomura, E. T.; Lee, Y. J.; Scheidt, W. R. *Inorg. Chem.* **1984**, *23*, 315.
(45) Helms, A. M.; Jones, W. D.; McLendon, G. L. *J. Coord. Chem.* **1991**, *23*, 351.
(46) Kokkou, S. C.; Rentzeperis, P. J. *Acta Crystallogr.* **1975**, *B31*, 2793.
(47) Eremenko, L. T.; Atovmyan, L. O.; Golovina, N. I.; Oreshko, G. O.; Fadeev, M. A. *Izv. Akad. Nauk. SSSR. Ser. Khim.* **1988**, 1870.
(48) Lianis, P. S.; Alexandrou, N. E. *Chim. Chron., New Ser.* **1984**, *13*, 193.
(49) Oreshko, G. O.; Fadeev, M. A.; Lagodzinskaya, G. V.; Kozyreva, I. Y.; Eremenko, L. T. *Izv. Akad. Nauk. SSSR. Ser. Khim.* **1986**, 2533.
(50) Kukushkin, V. Y.; Belsky, V. K.; Aleksandrova, E. A.; Konovalov, V. E.; Kirakosyan, G. A. *Inorg. Chem.* **1992**, *31*, 3836.
(51) Brokenshire, J. L.; Robert, J. R.; Ingold, K. U. *J. Am. Chem. Soc.* **1972**, *94*, 7040.
(52) Larson, H. O. In *The chemistry of functional groups*; Feuer, H., Ed; John Wiley & Sons: New York, 1969; Vol. 1, pp 304, 339 and references therein.
(53) Mlodnicka, T. In *Metalloporphyrins in Catalytic Oxidations*; Sheldon, R. A., Ed; Marcel Dekker Inc.: New York, 1994; p 261.

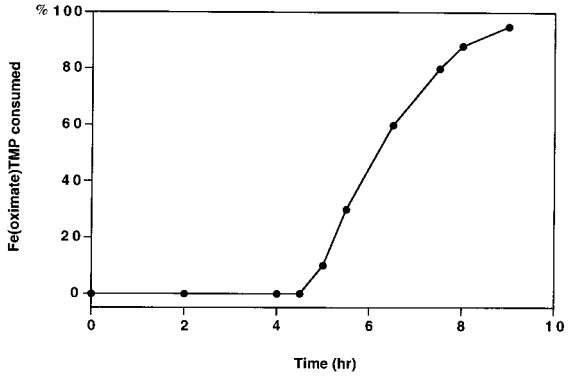


**Figure 4.** Time course plot of the aerobic oxidation of Fe(oximate)-TMP in benzene-$d_6$ as monitored by $^1$H NMR spectrosopy. The reaction was conducted by stirring a 0.75 mM Fe(oximate)TMP solution under 500 psi $O_{2(g)}$ at 25 °C in the dark. Note that each point on the plot represents an individual experiment.

from 14.7 to 100, 200, and 500 psi, the induction time was shortened from 2 weeks to 50, 20, and 4.5 h, respectively. Further, the oxidation phase lasted for 2 weeks at 14.7 psi $O_2$, while at 500 psi $O_2$ it was shortened to 5 h. These results suggest that $O_2$ directly participates in both the induction and the fast phase oxidation.

The rate of the aerobic oxidation of Fe(III)(oximate)P varied with the structure of the iron porphyrin. $^1$H NMR spectra of reaction mixtures showed that the 0.8 mM benzene-$d_6$ solutions of Fe(oximate)TPFPP were oxidized under 500 psi $O_2$ with an induction time of 3.5 h, and the overall oxidations was complete within 7 h. As in the aerobic oxidation of Fe(oximate)TMP, the organic products of the aerobic oxidation of Fe(oximate)-TFPP in benzene-$d_6$ were fluorenone (>70%) and the fluorene-based dimer (<30%). The porphyrin products were Fe(NO)-TPFPP (20%), $\mu$-oxoFe(III)TPFPP dimer (<5%),[54] and Fe($NO_3$)-TPFPP (75%). By contrast, Fe(oximate)TDCPP (**3**) showed no indication of aerobic oxidation in a variety of solvents, apparently due to precipitation.

**Origin of the Fluorenone Oxygen.** The oxygen atom of the fluorenone generated from the $O_2$-effected oxidation of Fe(oximate)P was verified to be derived from $O_2$. Because of the simplicity of the reaction, the potential oxygen sources can only be $O_2$, $H_2O$, or the oxime ligand. Two sets of $^{18}$O-labeling experiments were conducted to determine the oxygen source of fluorenone. A 2 mM benzene-$d_6$ solution of **2** was mixed with 1 $\mu$L of $H_2{}^{18}O$ (98% enriched, ~30 equiv with respect to **2**), and the reaction was brought to 100 psi $^{16}O_{2(g)}$. The second reaction contained the same solution of **2** except without $H_2{}^{18}O$, and the reaction was conducted under 100 psi $^{18}O_{2(g)}$ (98% enriched). Both reaction mixtures were stirred in the dark for 4 days before the reactions were stopped by releasing the headspace $O_2$ pressure. GC−MS spectrometric analysis showed that more than 75% of the fluorenone generated from the $^{18}O_2$-effected oxidation of **2** contained $^{18}$O. (Table 4). By contrast,

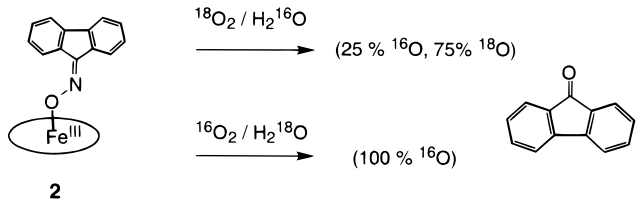


(54) Jayaraj, K.; Gold, G. E.; Toney, G. E.; Helms, J. H.; Hatfield, W. E. *Inorg. Chem.* **1986**, *25*, 3516.

**Table 4.** Mass Spectrometric Data of Fluorenone Generated from the $O_2$-Effected Oxidation of Fe(oximate)TMP[a]

| *m/e* | fluorenone from $^{16}O_2$[b] (%) | fluorenone from $^{18}O_2$[c] (%) |
|---|---|---|
| 179 | 0.4[d] | 0.0 |
| 180 | 100.0 | 30.5 |
| 181 | 13.8 | 5.9 |
| 182 | 0.8 | 100.0 |
| 183 | 0.0 | 15.2 |
| 184 | 0.0 | 1.0 |

[a] The reaction was conducted in a 2 mM benzene-$d_6$ solution of Fe(oximate)TMP under 100 psi $O_{2(g)}$ at 25 °C for 4 days. [b] Relative intensities of the mass spectrum of fluorenone generated from the reaction conducted under 100 psi regular $O_{2(g)}$. [c]Relative intensities of the mass spectrum of fluorenone generated from the reaction conducted under 100 psi $^{18}O_{2(g)}$.

the reaction conducted under $^{16}O_{2(g)}$ and $H_2{}^{18}O$ generated fluorenone containing only $^{16}$O. These results prove that $O_2$ is the predominant oxygen source of the fluorenone product, a characteristic similar to what has been observed in the NOS reaction.[22]

**Reaction of Fe(III)(oximate)P with CO.** The reaction of **2** and CO, an $O_2$ surrogate, was investigated. Complex **2** was found to react with $CO_{(g)}$ in benzene to generate Fe(CO)TMP and Fe($CO)_2$TMP within a few hours (Scheme 3). The $^1$H NMR resonance signals of **2** gradually converted ($t_{1/2} \approx 2$ days at 25 °C) to two sets of resonance signals of diamagnetic products under a slight excess of $CO_{(g)}$. One set of signals was identical to those of the authentic Fe($CO)_2$TMP/Fe(CO)TMP mixture prepared according to the literature method.[55] The other set of signals first appeared as broad bands, which gradually converted to the sharp signals of fluorenone oxime. Interestingly, the conversion of the signals took place ~2 days after the emergence of the Fe($CO)_2$TMP/Fe(CO)TMP signals.

Significantly, the rates of the formation of Fe(CO)P/Fe($CO)_2$P from Fe(oximate)P and CO for several porphyrins paralleled the redox potentials of the corresponding Fe(III)P species. The order of the reduction potentials of the corresponding Fe(III)P species is as follows (e.g., with $Cl^-$ as the axial ligand): Fe-(Cl)TPFPP (−0.08 V vs SCE in $CH_2Cl_2$)[56] > Fe(Cl)TDCPP (−0.221 V)[57] > Fe(Cl)TMP (−0.49 V).[58] Consistent with this trend, the order of the reaction rates of Fe(oximate)P and 1 atm $CO_{(g)}$ was found to be as follows: Fe(oximate)TPFPP ($t_{1/2}$ = 10 min at 25 °C) > Fe(oximate)TDCPP (**3**) ($t_{1/2}$ = 30 min) > Fe(oximate)TMP (**2**) ($t_{1/2}$ = 1.5 h). This correlation suggests that the rate-limiting step of the formation of Fe(CO)P involves the reduction of Fe(III)P to Fe(II)P.

**Scheme 3**

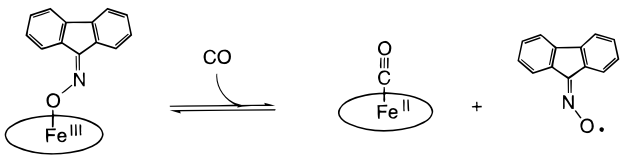


The kinetics of the reaction of Fe(oximate)P and $CO_{(g)}$ have been investigated in detail to further reveal the reaction mechanism. Thus, the formation rates of Fe($CO)_2$TMP from **2** and 1 atm $CO_{(g)}$ were measured at temperatures ranging from

(55) Wayland, B. B.; Mehne, L. F.; Swartz, J. *J. Am. Chem. Soc.* **1978**, *100*, 2379.

(56) Grinstaff, M. W.; Hill, M. G.; Birnbaum, E. R.; Schaefer, W. P.; Labinger, J. A.; Gray, H. B. *Inorg. Chem.* **1995**, *34*, 4896.

(57) Chen, H. L.; Ellis, P. E., Jr.; Wijesekera, T.; Hagan, T. E.; Groh, S. E.; Lyons, J. E.; Ridge, D. P. *J. Am. Chem. Soc.* **1994**, *116*, 1086.

(58) Swistak, C.; Mu, X. M.; Kadish, K. M. *Inorg. Chem.* **1987**, *26*, 4360.

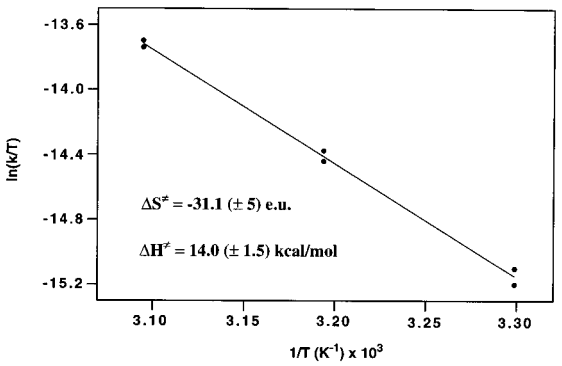


**Figure 5.** Eyring plot for the generation of Fe(CO)TMP/Fe(CO)$_2$TMP from a benzene solution of Fe(oximate)TMP (7 $\mu$M) under 1 atm $CO_{(g)}$. The *k* values are the pseudo-first-order rate constants of the increase of Fe(CO)$_2$TMP (monitored at 426 nm) at 30, 40, and 50 °C in the dark. The correlation coefficient (*r*) of the data is 0.998.

30 to 50 °C, and an Eyring plot was constructed based on the pseudo-first-order rate constants (Figure 5). From this Eyring plot, the enthalpy ($\Delta H^{\ddagger}$) and the entropy of activation ($\Delta S^{\ddagger}$) of the reaction were calculated to be 14.0(±1.5) kcal/mol and −31.1(±5.0) eu, respectively. The large, negative entropy term indicates that the rate-limiting step of the reaction involves an *association* of the reactants.[59] Consistent with this notion, the formation rate of Fe(CO)P/Fe(CO)$_2$P from Fe(oximate)P and CO was found to be directly proportional to the partial pressure of $CO_{(g)}$ above the reaction mixture.[60] On the basis of these results, the rate law for the formation of Fe(CO)TMP is shown as eq 3,[61] where $k = 1.04\ (\pm\ 0.09) \times 10^{-1}\ M^{-1}\ s^{-1}$ at 30 °C.

$$-\mathrm{d[Fe(oximate)TMP]}/\mathrm{d}t = k\mathrm{[Fe(oximate)TMP][CO]} \quad (3)$$

In light of the $\Delta S^{\ddagger}$ value, the dependence of Fe(CO)P formation rates on both of the reduction potentials of Fe(III)P and headspace $CO_{(g)}$ partial pressures, we conclude that Fe(CO)P was generated via the CO-induced reduction of Fe(oximate)P. In the rate-limiting step, CO would approach Fe(oximate)P from the direction trans to the oximate ligand, which was induced to dissociate from **2**. The generation of Fe(CO)P indicates that Fe(oximate)P was reduced to Fe(II)P either during or after the dissociation of the oximate ligand. Since CO can only reduce Fe(III)P in aqueous solutions,[62] it is unlikely that CO could reduce Fe(III)(oximate)P to form Fe(II)P. Thus, Fe(CO)P/Fe(CO)$_2$P must come from the reaction of CO and Fe(II)P, which would result from the homolysis of the Fe−O bond of Fe(oximate)P. Hence, CO induces the Fe−O bond homolysis via a mechanism similar to the $\pi$-acid-assisted reduction of Fe(III)P by phosphine[63,64] or isocyanide.[65]

Such a homolysis of the Fe−O bond of Fe(oximate)TMP would also generate the fluorenyl iminoxy radical. However, the fluorenyl iminoxy radical dimerization product, **1**, was not detected in the products under these conditions. Instead, free fluorenone oxime was found as the final organic product 2 days after the emergence of Fe(CO)TMP/Fe(CO)$_2$TMP. This delayed emergence of fluorenone oxime in the reaction product suggests that it derived from the decomposition of reaction intermediates, such as adducts of CO and fluorenyl iminoxy radicals. One likely intermediate is bis(fluorenoneoximyl)carbonate resulted from the free-radical carbonylation of fluorenyl iminoxy radical and CO.[66] The slow hydrolysis of this carbonate species by the residual water in the sample would generate fluorenone oxime and carbonic acid (eq 4). Indeed, this transformation consumed

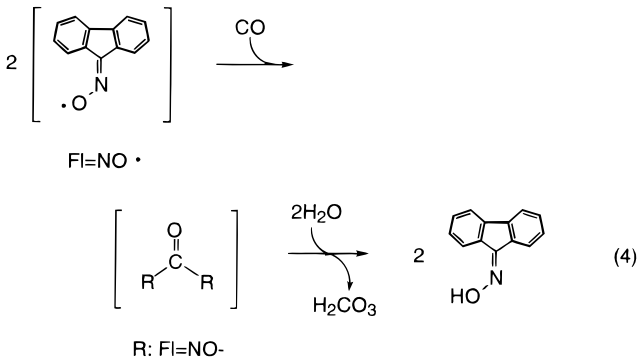


(4)

the residual water in the benzene-$d_6$ solution as was evident by the diminishing of the $^1$H NMR resonance signal of water in the reaction mixtures.

In analogy to the reaction of CO and Fe(oximate)P, the $\pi$-acid NO also induced the Fe−O bond homolysis of Fe(oximate)P. $^1$H NMR analysis showed that a 2 mM benzene-$d_6$ solution of **2** reacted with a substoichiometric amount of $NO_{(g)}$ to generate Fe(NO)TMP as the only iron porphyrin product. This reaction was so fast that it took place even when $NO_{(g)}$ was added to a solution of **2** under argon purging. Concomitant with the formation of Fe(NO)TMP, the oximate ligand of **2** was converted to a one-to-one ratio of fluorenone oxime and the fluorene-based dimer **1** in addition to trace amounts of fluorenone.

In summary, we have presented the first example of synthetic iron porphyrin-catalyzed oxidation of oximes by $O_2$. This reaction is analogous to the $O_2$-effected oxidation of the oximate ligand of Co(III)(salen) reported by Nishinaga.[67] The proposed mechanism for that reaction involved the insertion of $O_2$ between Co(II) and an iminoxy radical. The long induction time of the $O_2$-effected oxidation of Fe(oximate)P suggests that its rate-limiting step is the homolysis of the Fe−O bond, which would generate fluorenyl iminoxy radical and Fe(II)P. Among the several mechanisms that could accommodate our data, the most probable one is the reaction of Fe(II)P, fluorenyl iminoxy radical, and $O_2$. This reaction would furnish an unstable peroxyFe(III)P intermediate (**4**) in analogy to the cobalt salen case (Scheme 4). If compound **4** were to decompose via O−O bond homolysis, analogously to the decomposition of other alkylperoxyFe(III)P species,[68,69] fluorenone, NO, and an oxoFe(IV) porphyrin would be generated in a single step. NO would be captured by either Fe(II)P or Fe(oximate)P to afford Fe-

(59) Wilkins, R. G. *Kinetics and mechanism of reactions of transition metal*, 2nd ed.; VCH Publishers, Inc.: New York, 1991.

(60) When the reaction was conducted under 1 atm 20/80 CO/Ar gas mixture, the formation rate of Fe(CO)TMP/Fe(CO)$_2$TMP was reduced to 18(±2)% of that of the reaction conducted at 1 atm $CO_{(g)}$.

(61) The second-order rate constant was calculated from the pseudo-first-order rate constant of the formation of Fe(CO)TMP [$(8 \pm 0.4) \times 10^{-5}$ $s^{-1}$] at 30 °C and the concentration of CO in benzene (7.37−8.05 mM) (Cargill, R. W. In *Carbon Monoxide*; Cargill, R. W., Ed.; Pergamon Press: New York, 1981; Vol. 43, p 114).

(62) Bickar, D.; Bonaventura, C.; Bonaventura, J. *J. Biol. Chem.* **1984**, *259*, 10777.

(63) Inoue, H.; Akahori, H.; Ohno, Y.; Nakazawa, K.; Nonomura, Y.; Yoshioka, N.; Heckmann, G.; Fluck, E. *Z. Naturforsch. Sect. B* **1995**, *50*, 1222.

(64) Del Gaudio, J.; La Mar, G. N. *J. Am. Chem. Soc.* **1978**, *100*, 1112.

(65) Nakano, T.; Kitamura, Y. *Chem. Lett.* **1989**, 1207.

(66) Ryu, I.; Sonoda, N. *Angew. Chem., Int. Ed. Engl.* **1996**, *35*, 1050.

(67) Nishinaga, A.; Yamazaki, S.; Miwa, T.; Matsuura, T. *React. Kinet. Catal. Lett.* **1991**, *43*, 273.

(68) Balch, A. L.; Cornman, C. R.; Safari, C. R.; Latos-Grazynski, L. *Organometallics* **1990**, *9*, 2420.

(69) Balch, A. L.; Hart, R. L.; Latos-Grazynski, L.; Traylor, T. G. *J. Am. Chem. Soc.* **1990**, *112*, 7382.

**Scheme 4**

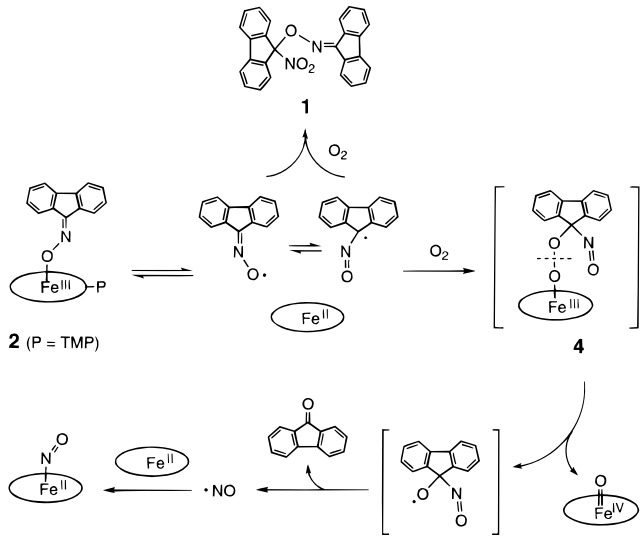

(NO)P. Further oxidation of Fe(NO)P would lead to Fe($NO_3$)P and the putative Fe(ONO)P as is observed.

**Implications for the NOS Reaction Cycle.** The implications of this model to the NOS reaction mechanism are intriguing. First, the structure of the Fe(III) oximate **3** suggests an unprecedented mode of interaction between the NOS Fe(III) heme and the *N*-hydroxyguanidine function of NHA. This notion is unusual given the fact that there is no evidence of an Fe−O bond in the NHA-bound NOS.[70,71] Nonetheless, the crystal structure of L-arginine-bound iNOS shows that the guanidine-N of arginine is 3.8 Å away from the heme-iron. This distance is only ∼1 Å longer than that observed for Fe and oximyl-N in **3**. Further, the NHA-bound iNOS has been found to have a similar structure with the *N*-hydroxy oxygen positioned directly above the heme iron.[72] Movement of NHA within the active site of NOS could allow the *N*-hydroxy group to approach and ligate to Fe(III) heme. Second, the occurrence of the Fe−O bond homolysis of Fe(oximate)P under CO suggests that NHA is able to reduce the Fe(III) heme to initiate the second step of the NOS reaction. This notion is even more convincing when one considers the redox potentials of the NOS Fe(III) heme ($E°$= −248 to ∼−263 mV)[73] and the conjugate base of the NHA *N*-hydroxy group ($E° \leq -200$ mV).[74] Thus, the Fe−O homolysis of the presumed NHA−Fe(III) heme adduct could be an energetically accessible process.

There have been reports suggesting that *N*-hydroxyarginine does not reduce Fe(III) heme to initiate the second step of NOS reaction.[20,75] It has been shown that the reaction of NOS and NHA under $CO_{(g)}$ does not give the characteristic P450-type visible spectrum ($\lambda_{max}$ = 450 nm).[75] One possible reason for this negative result is that the equilibrium concentration of the CO-ligated Fe(II) heme relative to Fe(III) heme is too low to be detected by the difference spectrum technique, for it has been shown that tetrahydrobiopterin ($H_4B$) and L-arginine restrict CO access to NOS heme iron. Due to this steric restriction, NOS Fe(II) heme has a lower affinity to CO than other hemoproteins.[76] The binding constant of iNOS Fe(II) heme, the isoform used in the CO binding assay by Pufahl et al., toward CO ($K^{co}$) is $5 \times 10^3$ $M^{-1}$,[77] 16 times smaller than those of other P450 monoxygenases such as P450cam and P450nor ($K^{co}$= $8.5 \times 10^4$ and $8.8 \times 10^4$ $M^{-1}$, respectively).[78] Therefore, unless the majority of the iNOS sample is reduced to Fe(II) and the solution contains high concentration of CO, the UV−visible signal of thiolate-ligated NOS Fe(II)(CO) heme species would be difficult to detect.

Another likely reason for the absence of a P-450-type difference spectrum is that the NHA-ligated 6-coordinate heme−Fe(III) species could be in an equilibrium with the tightly associated iminoxy radical−Fe(II) heme so that the Fe(II) heme cannot react with CO. The NHA-derived iminoxy radical ligand may associate with the Fe(II) heme so strongly that the complex only decomposes upon reacting with $O_2$ at the carbon center of that radical. Similar tightly associated Fe(III)−substrate adducts have been shown to be involved in both of the intradiol-cleaving catechol dioxygenase and α-keto acid-dependent oxygenase reactions.[79,80]

We suggest that the second step of the NOS reaction to form NO is initiated by an Fe−O bond homolysis of the NHA−Fe(III) heme adduct. This process would generate an Fe(II) heme and the NHA-derived iminoxy radical. The reaction of these two species with $O_2$ would reasonably afford the key peroxyFe(III) heme species (an analogue of **4**) followed by its decomposition to citrulline, NO, and oxoFe(IV) heme. The single NADPH-derived reducing equivalent consumed in the second step NOS reaction would then be used to reduce oxoFe(IV) heme back to Fe(III) heme. In light of the direct contact of the potential 1-electron cofactor $H_4B$[81a] and NOS heme,[82] it is likely in this scenario that $H_4B$ is responsible for mediating this reduction process affording an intermediate $H_3B^{\bullet}$ radical[81b] (Scheme 5). Such a scheme has the intuitively attractive features of producing a radical species, NO, via the participation of single-electron redox cofactors, $H_4B$ and an NADPH-derived reducing equivalent, by an radical-type autoxidation process. This and other aspects of this interesting reaction are under current study.

## Experimental Section

**General Procedures and Methods.** NMR spectra were collected on JEOL GSX-270 (270 MHz) and Varian INOVA 500 (500 MHz) NMR spectrometers. $^1$H NMR chemical shift values are reported in ppm relative to the residual solvent resonances ($^1$H NMR $\delta$ 7.26 for $C_6HD_5$). UV−visible experiments were conducted on an HP 8452A diode array spectrophotometer and a Varian Cary 2390 spectrophotometer. GC−MS data were obtained on an HP 5890 series II Plus gas chromatograph equipped with a HP-5MS capillary column (30 m) and an HP 5989B mass spectrometer. All anaerobic and gas-control experiments were conducted either on a high-vacuum ($<10^{-6}$ mmHg) Schlenk preparative line or in an inert-air glovebox controlled by

(70) Salerno, J. C.; Martasek, P.; Williams, R. F.; Masters, B. S. S. *Biochemistry* **1997**, *36*, 11821.
(71) Sennequier, N.; Stuehr, D. J. *Biochemistry* **1996**, *35*, 5883.
(72) Tainer, J. A., personal communication on the crystal structure of iNOS oxygenase dimer with bound cofactors and NHA.
(73) Presta, A.; Weber-Main, A. W.; Stankovich, M. T.; Steuhr, D. J. *J. Am. Chem. Soc.* **1998**, *120*, 9460.
(74) Bordwell, F. G.; Ji, G.-Z. *J. Org. Chem.* **1992**, *57*, 3019.
(75) Pufahl, R. A.; Marletta, M. A. *Biochem. Biophys. Res. Commun.* **1993**, *193*, 452.
(76) Wang, J. L.; Stuehr, D. J.; Rousseau, D. L. *Biochemistry* **1997**, *36*, 4595.
(77) Abu-Soud, H. M.; Wu, C. Q.; Ghosh, D. K.; Stuehr, D. S. *Biochemistry* **1998**, *37*, 3777.
(78) Shiro, Y.; Minoru, K.; Iizuka, T.; Nakahara, K.; Shoun, H. *Biochemistry* **1994**, *33*, 8673.
(79) Bugg, T. D.; Winfield, C. J. *Nat. Prod. Rep.* **1998**, *15*, 513.
(80) Que, L., Jr.; Ho, R. Y. N. *Chem. Rev.* **1996**, *96*, 2607.
(81) (a) Lunte, C. E.; Kissinger, P. T. *Anal. Chem.* **1983**, *55*, 1458. (b) The $H_3B^{\bullet}$ radical has very recently been detected in a single-turn-over experiment with the iNOS heme domain: Hurshman, A. R.; Krebs, C.; Edmondson, D. E.; Huynh, B. H.; Marletta, M. A. *Biochemistry* **1999**, *38*, 15689−15696.
(82) Crane, B. R.; Arvai, A. S.; Ghosh, D. K.; Wu, C.; Getzoff, E. D.; Stuehr, D. J.; Tainer, J. A. *Science* **1998**, *279*, 2121.

**Scheme 5**

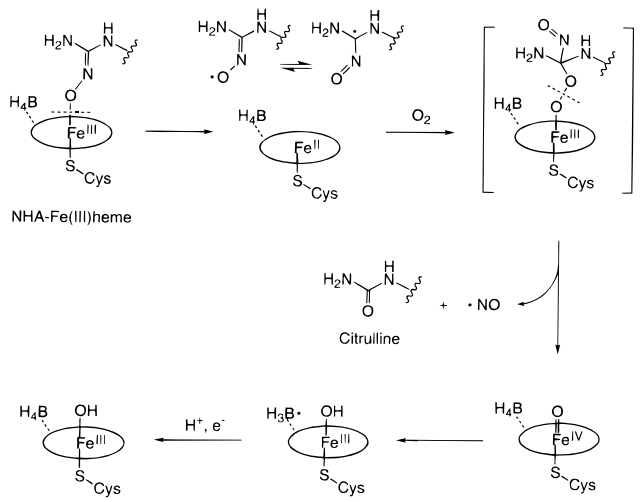


Vacuum Atmosphere Co. Dri-Train model MO40-2 with $O_2$ concentration maintained under 2 ppm.

**Materials.** All reagents and chemicals were obtained from commercial sources and used as received unless otherwise described. Solvents were dried and distilled under $N_2$ immediately before use according to literature procedures.[83] Fluorenone oxime was prepared by refluxing a mixture of hydroxylamine hydrochloride and fluorenone in ethanol.[84] The $^{15}$N-labeled fluorenone oxime was prepared from $^{15}N$-hydroxylamine hydrochloride (> 96% $^{15}$N enriched). Fe(III)tetrakis-(mesityl)porphyrin chloride (Fe(Cl)TMP), Fe(III)tetra(pentafluorophenyl)-porphyrin chloride (Fe(Cl)TPFPP), and Fe(III)tetra(2,6dichlorophenyl)-porphyrin chloride (Fe(Cl)TDCPP) were purchased from Midcentury Inc. and used directly without further purification. $^{18}O_{2(g)}$ (98% enriched) and $H_2{}^{18}O$ (98% enriched) were both purchased from Cambridge Isotope Laboratories. C. P. grade $NO_{(g)}$ and $CO_{(g)}$ were purchased from Matheson Gas Products. $NO_{(g)}$ was passed through a column of KOH pellets to remove higher nitrogen oxides immediately before use.

**Hydroxo(5,10,15,20-tetrakis(mesityl)porphyrinato)iron(III) [Fe-(OH)TMP].**[85] A total of 10 mg of Fe(Cl)TMP dissolved in minimum amount of $CH_2Cl_2$ was eluted through a column packed with a mixture of basic alumina and water (10 wt %) with purified $CH_2Cl_2$. The solvent was immediately removed in vacuo from the green elute to give quantitative a yield of Fe(OH)TMP: $^1$H NMR ($C_6D_6$, 25 °C, 270 MHz) $\delta$ 78 (8H, pyrrole H), 11 (s, 4H, *m*-phenyl H), 12 (s, 4H, *m*-phenyl H), 3.3 (s, 12H, *p*-methyl H), 2−6 (broad, 24H, *o*-methyl H); UV−visible ($C_6H_6$) $\lambda_{max}$ ($\epsilon \times 10^{-3}$) 346 (30), 416 (98), 510 nm (11).

**Hydroxo(5,10,15,20-tetrakis(pentafluorophenyl)porphyrinato)-iron(III) [Fe(OH)TPFPP]** was prepared with the same procedure above using Fe(Cl)TPFPP instead of Fe(Cl)TMP. The eluate containing Fe-(OH)TPFPP was immediately reduced to dryness to avoid the formation of the $\mu$-oxo dimer:[54] UV−visible ($CH_2Cl_2$) $\lambda_{max}$ ($\epsilon \times 10^{-3}$) 406 (76), 563 nm (11.9).

**Hydroxo(5,10,15,20-tetrakis(2,6-dichlorophenyl)porphyrinato)-iron(III) [Fe(OH)TDCPP]** was prepared with the same procedure above using Fe(Cl)TDCPP instead of Fe(Cl)TMP: UV−visible ($CH_2Cl_2$) $\lambda_{max}$ 332, 414, 578 nm.

**Nitrato(5,10,15,20-tetrakis(mesityl)porphyrinato)iron(III) [Fe-($NO_3$)TMP]** was prepared by modification of the literature method[32] by mixing a one-to-one ratio of Fe(OH)TMP and $HNO_3$ in benzene-$d_6$. The progress of the reaction was monitored by $^1$H NMR. The signals for Fe(OH)TMP were completely converted to another Fe(III)TMP species upon the mixing. On the basis of the literature precedent and the stoichiometry of the reaction, the new Fe(III)P was assigned as Fe($NO_3$)TMP: $^1$H NMR ($C_6D_6$, 25 °C, 270 MHz) $\delta$ 79 (8H, pyrrole H), 15.2 (s, 4H, *m*-phenyl H), 16.4 (s, 4H, *m*-phenyl H), 4.0 (s, 12H, *p*-methyl H),2−6 (broad, 24H, *o*-methyl H); UV−visible ($C_6H_6$) $\lambda_{max}$ ($\epsilon \times 10^{-3}$) 330 (67), 418 (100), 580 nm (7.7).

**Nitrato(5,10,15,20-tetrakis(pentafluorophenyl)porphyrinato)iron-(III) [Fe($NO_3$)TPFPP]** was prepared with the same procedure above using Fe(OH)TPFPP instead of Fe(OH)TMP: $^1$H NMR ($C_6D_6$, 25 °C, 270 MHz) $\delta$ 81 (pyrrole H); UV−visible ($C_6H_6$) 408, 507 nm.

**Nitrosyl(5,10,15,20-tetrakis(mesityl)porphyrinato)iron(II) [Fe-(NO)TMP]** was prepared by reductive nitrosylation of Fe(Cl)TMP.[86,87] NO gas was introduced to the anaerobic benzene solution of a 1:1 mixture of methanol and Fe(Cl)TMP. The solution was reduced to dryness after reacting for overnight. The solid product was isolated under ambient air: $^1$H NMR ($C_6D_6$, 25 °C, 270 MHz) $\delta$ 2.60 (s, 8H, *p*-methyl H), 2.1−2.8 (24H, *o*-methyl H), 5.6−6.4 (8H, pyrrole H), 7.8−8.6 (8H, *m*-phenyl H); UV−visible ($CH_2Cl_2$) $\lambda_{max}$ ($\epsilon \times 10^{-3}$) 408 (92), 539 (11), 611 nm (2.3); IR (KBr) $\nu_{NO}$ 1677 cm$^{-1}$(vs).

**Nitrosyl(5,10,15,20-tetrakis(mesityl)porphyrinato)iron(II) [Fe-(NO)TPFPP]** was prepared with the same procedure above using Fe-(Cl)TPFPP instead of Fe(Cl)TMP: $^1$H NMR ($C_6D_6$, 25 °C, 270 MHz) $\delta$ 5.4−6. 6 (pyrrole H); UV−visible ($C_6H_6$) 402, 544 nm.

**Monocarbonyl(5,10,15,20-tetrakis(mesityl)porphyrinato)iron-(II) and Biscarbonyl(5,10,15,20-tetrakis(mesityl)porphyrinato)iron-(II) [Fe(CO)TMP and Fe($CO)_2$TMP]** were prepared from Fe(II)TMP and $CO_{(g)}$.[55] Fe(II)TMP was prepared by reducing Fe(Cl)TMP with sodium dithionite in benzene/$H_2O$ under $N_2$. The mixture was stirred until all Fe(III)TMP was consumed. The organic layer was separated from the aqueous layer under CO to generate a mixture of Fe(CO)-TMP/Fe($CO)_2$TMP. The UV−visible spectrum of the crude mixture under CO showed that, upon either heating or irradiation, the 410 nm peak increases while the 426 nm peak decreases. Due to the instability of the second CO ligand, the species giving the 426 nm peak was assigned as Fe($CO)_2$TMP while the species giving the 410 nm peak was assigned as Fe(CO)TMP: $^1$H NMR ($C_6D_6$, 25 °C, 270 MHz) $\delta$ 1.95 (s, 24H, *o*-methyl H), 2.43 (s, 12H, *p*-methyl H), 7.09 (s, 8H, *m*-phenyl H), 8.79 (s, 8H, pyrrole H); UV−visible ($CH_2Cl_2$) $\lambda_{max}$ Fe($CO)_2$TMP 426, 510 nm; Fe(CO)TMP 410, 502 nm.

**Fluorenoneoximato(5,10,15,20-tetrakis(mesityl)porphyrinato)-iron(III) [Fe(oximate)TMP] (2).** Ten milligrams of Fe(OH)TMP (11.7 $\mu$mol) and 2.4 mg of fluorenone oxime (12.2 $\mu$mol) were mixed in 20 mL of benzene. The mixture was stirred for 10 min, and then the solvent was removed in vacuo. The solid was dissolved in a minimum of $CHCl_3$, and $CH_3CN$ was diffused in over 2 days to precipitate small crystals of **2**: $^1$H NMR ($C_6D_6$, 25 °C, 270 MHz) $\delta$ 78 (8H, pyrrole H). 12.5 (s, 4H, *m*-phenyl H), 11.7 (s, 4H, *m*-phenyl H), 16.6 (s, 1H), 14.7 (s, 1H), 10.5 (s, 1H), 9.2 (s, 1H), −20 (s, 1H), −25 (s, 1H), −30 (s, 1H); UV−visible ($CH_2Cl_2$) $\lambda_{max}$ ($\epsilon \times 10^{-3}$) 332 (51), 422 (102), 580 (12), 636 nm (7.5).

**Fluorenoneoximato(5,10,15,20-tetrakis(2,6-dichlorophenyl)por-phyrinato)iron(III) [Fe(oximate)TDCPP]** was prepared with the same procedure above using Fe(OH)TDCPP instead of Fe(OH)TMP: $^1$H NMR ($C_6D_5Cl$, 25 °C, 270 MHz) $\delta$ 76 (8H, pyrrole H), 11.5 (s, 4H, *m*-phenyl H), 10.8 (s, 4H, *m*-phenyl H), 7.9 (s, 4H, *p*-phenyl H), 17.1 (s, 1H), 15.6 (s, 1H), 9.7 (s, 1H), −17 (s, 1H), −21 (s, 1H), −28 (s, 1H); UV−visible ($CH_2Cl_2$) $\lambda_{max}$ 338, 416, 578 nm.

**Fluorenoneoximato(5,10,15,20-tetrakis(pentafluorophenyl)por-phyrinato)iron(III) [Fe(oximate)TPFPP]** was prepared with the same procedure above using Fe(OH)TPFPP instead of Fe(OH)TMP: $^1$H NMR ($C_6D_6$, 25 °C, 270 MHz) $\delta$ 79 (8H, pyrrole H), 17.5 (s, 1H), 16.7 (s, 1H), 11.4 (s, 1H), 10.3 (s, 1H), −16 (s, 1H), −22 (s, 1H) −29 (s, 1H); UV−visible ($CH_2Cl_2$) $\lambda_{max}$ ($\epsilon \times 10^{-3}$) 404 (76), 570 nm (10.8).

***O*-(9-Nitro-9-fluorenyl)fluorenone Oxime.** Four milligrams of Fe-(OH)TDCPP and 27 mg of fluorenone oxime were dissolved in 100 mL of thiophene-free benzene in a silanized Pyrex flask. The solution was bubbled with $O_2$ and irradiated with a 200 W tungsten lamp filtered with a No. 3-73 Corning color glass filter ($\lambda$ > 420 nm). After fluorenone oxime completely reacted (~3 days), the solvent was removed in vacuo. The solid was triturated with $CH_3CN$, and the pale yellow insoluble residue was isolated. Yield is 50% based on fluorenone

(83) Perrin, D. D. *Purification of Laboratory Chemicals*, 3rd ed.; Pergamon Press: Oxford, U.K., 1988.
(84) *Vogel's Textbook of Practical Organic Chemistry*, 4th ed.; Furniss, B., Hannaford, A. J., Rogers, V., Smith, P. W. G., Tatchell, A. R., Eds; Wiley: New York, 1987; p 1113.
(85) Groves, J. T.; Gross, Z.; Stern, M. K. *Inorg. Chem.* **1994**, *33*, 5065.
(86) Wayland, B. B.; Olson, L. W. *J. Am. Chem. Soc.* **1974**, *96*, 6037.
(87) Mu, X. H.; Kadish, K. M. *Inorg. Chem.* **1988**, *27*, 4720.

oxime: $^1$H NMR ($C_6D_6$, 2mM, 25 °C, 500 MHz) $\delta$ 6.80 (t, $J$ = 7.5 Hz, 1H, 2-fluorenoneoximyl H), 6.93 (t, $J$ = 7.5 Hz, 1H, 7-fluorenoneoximyl H), 6.95 (t, $J$ = 7.5 Hz, 1H, 3-fluorenoneoximyl H), 6.97 (t, $J$ = 7.5 Hz, 2H, 2-fluorenyl H), 7.01 (t, $J$ = 7.5 Hz, 1H, 6-fluorenoneoximyl H), 7.06 (t, $J$ = 7.5 Hz, 1H, 3-fluorenyl H), 7.11 (d, $J$ = 7.5 Hz, 1H, 4-fluorenoneoximyl H), 7.12 (d, $J$ = 7.5 Hz, 1H, 5-fluorenoneoximyl H), 7.20 (d, $J$ = 7.5 Hz, 2H, 4-fluorenyl H), 7.64 (d, $J$ = 7.5 Hz, 1H, 8-fluorenoneoximyl H), 8.02 (d, $J$ = 7.5 Hz, 2H, 1-fluorenyl H), 8.30 (d, $J$ = 7.5 Hz, 1H, 1-fluorenoneoximyl H); IR ($CDCl_3$) $\nu_{NO2}$ 1561 (vs), 1349 (s); $\nu_{NO}$ 989 (vs); $\nu_{CO}$ 1036 cm$^{-1}$ (s).

**X-ray Crystallography. General Procedure.** X-ray crystallographic studies were carried out on a Nonius KappaCCD diffractometer equipped with graphite-monochromatized Mo K$\alpha$ radiation ($\lambda$ = 0.710 73 Å). Samples were either mounted on a glass fiber with epoxy cement or sealed in a glass capillary, and the diffraction data were collected at room temperature. Relevant crystallographic information is listed in Table 1.

**X-ray Crystal Structure Determination of *O*-(9-Nitro-9-fluorenyl)fluorenone Oxime (1).** Single crystals of **1** suitable for X-ray crystallographic analysis were obtained by slow diffusion of $CH_3CN$ into a benzene solution of **1** over a period of 1 week. A pale yellow irregular chunk (0.15 mm × 0.20 mm × 0.25 mm in size) was used for the diffraction experiment (Table 1). A total of 608 frames of data were collected at 298(2) K with an oscillation range of 1°/frame and an exposure time of 120 s/deg.[88] A total of 26 402 reflections ($\theta_{max}$ = 22.48°) were indexed, integrated, and corrected for Lorentz and polarization effects using DENZO-SMN and SCALEPACK.[89] The $\theta_{max}$ limit was reduced from the standard 27.50° due to the sample being a poor scatterer. Data reduction yielded 2622 unique reflections ($R_{int}$ = 0.0530) of which 1948 had $I > 2\sigma(I)$. Postrefinement of the unit cell parameters gave $a$ = 9.8776(6) Å, $b$ = 11.9206(6) Å, $c$ = 17.4262(12) Å, $\beta$ = 101.550(3)°, and $V$ = 2010.3(2) Å$^3$. Axial photographs and systematic absences were consistent with the compound having crystallized in the monoclinic space group $P2_1/n$ (No. 14).

The structure was solved by direct methods and refined by full-matrix least squares on $F^2$ using SHELXTL.[90] All of the non-hydrogen atoms were refined with anisotropic displacement coefficients. The hydrogen atoms were assigned isotropic displacement coefficients $U$(H) = 1.2$U$(C), and their coordinates were allowed to ride on their respective carbons. Nearly 50% of the structure was found to be disordered. The disorder was treated with a two-site model as follows: [O(1), N(1), C(1), C(2), C(3), C(4), C(4A), C(4B), C(5), C(6), C(7), C(8), C(8A), C(9), C(9A)] and [O(1*), N(1*), C(1*), C(2*), C(3*), C(4*), C(4A*), C(4B*), C(5*), C(6*), C(7*), C(8*), C(8A*), C(9*), C(9A*)]. The partial atoms at these two sites were assigned occupancy factors of a half and the carbons refined with mild distance restraints. The weighting scheme employed was $w = 1/[\sigma^2(F_o^2) + (0.0551P)^2 + 0.7277P]$, where $P = (F_o^2 + 2F_c^2)/3$. The refinement converged to $R(F)$ = 0.0569, $wR(F^2)$ = 0.1407, and $S$ = 1.20 for 1948 reflections with $I > 2\sigma(I)$, and $R(F)$ = 0.0772, $wR(F^2)$ = 0.1529, and $S$ = 1.09 for 2622 unique reflections, 416 parameters, and 72 restraints. The maximum $\Delta/\sigma$ in the final cycle of leas -squares was less than 0.001, and the residual peaks on the final difference Fourier map ranged from −0.094 to 0.160 eÅ$^{-3}$. Scattering factors were taken from the *International Tables for Crystallography*, Volume C.[91,92]

**X-ray Crystal Structure Determination of Fe(oximate)TDCPP (3).** Single crystals of **3** suitable for X-ray crystallographic analysis were obtained by slow diffusion of *n*-heptane into a chlorobenzene solution of **3** over 3 days. A dark purple prism cut to 0.12 mm × 0.28 mm × 0.35 mm in size was used for the diffraction experiment (Table 1). A total of 493 frames of data were collected at 298(2) K with an oscillation range of 2°/frame and an exposure time of 60 s/deg.[88] A total of 79 647 reflections ($\theta_{max}$ = 27.46°) were indexed, integrated, and corrected for Lorentz and polarization effects using DENZO-SMN and SCALEPACK.[89] Data reduction yielded 13 775 unique reflections ($R_{int}$ = 0.0490) of which 7272 had $I > 2\sigma(I)$. Postrefinement of the unit cell parameters gave $a$ = 12.5029(2) Å, $b$ = 13.0424(4) Å, $c$ = 18.9793(5) Å, $\alpha$ = 81.701(1)°, $\beta$ = 88.304(2)°, $\gamma$ = 84.263(2)°, and $V$ = 3046.80(13) Å$^3$. Axial photographs and a lack of systematic absences suggested that the compound had crystallized in the triclinic space group $P1$ or $P\bar{1}$. The latter space group $P\bar{1}$ (No. 2) was selected on the basis of an observed mean value of 0.901 for $|E^* E - 1|$ (versus the expectation values of 0.968 and 0.736 for centric and noncentric data, respectively).

The structure was solved by direct methods and refined by full-matrix least squares on $F^2$ using SHELXTL[90] to $R(F)$ = 0.1545 and $wR(F^2)$ = 0.3066 for 13 775 unique reflections. A disordered chlorobenzene solvent molecule was included in the refinement, and two additional carbon atoms were placed at a second (presumably heptane) solvent site. The chlorobenzene did not refine well, and the identity of the second solvent molecule could not be assigned via a discrete-atom approach. Therefore, the analysis was resumed with the following solvent-free model.

The SQUEEZE/BYPASS procedure[93] implemented in PLATON[94] was used to account for the solvent electron density. Two solvent-accessible voids were detected. The first of these two voids is situated along the crystallographic $c$-axis (0, 0, $z$) and has a volume and electron count of 482 Å$^3$ and 92 $e$, respectively. From our discrete-atom approach mentioned above, we know that this void is occupied by two chlorobenzene molecules (339 Å$^3$, 116 $e$). The second void is situated at the center of the cell (0.5, 0.5, 0.5) and has a volume and electron count of 245 Å$^3$ and 55 $e$, respectively. These results suggest that the occupant of this second void may be a molecule of the precipitating solvent heptane (244 Å$^3$, 58 $e$) used in recrystallizing the iron complex. Since there are two molecules of the iron complex per cell, the chemical formulation $C_{57}H_{28}C_{l8}FeN_5O\cdot_6H_5Cl\cdot.5C_7H_{16}$ is proposed.

The SQUEEZE-processed data were used in all subsequent cycles of least squares. All of the nonhydrogen atoms were refined with anisotropic displacement coefficients. The hydrogen atoms were assigned isotropic displacement coefficients $U$(H) = 1.2$U$(C), and their coordinates were allowed to ride on their respective carbons. The weighting scheme employed was $w = 1/[\sigma^2(F_o^2) + (0.0838P)^2]$, where $P = (F_o^2 + 2F_c^2)/3$. The refinement converged to $R(F)$ = 0.0571, $wR(F^2)$ = 0.1490, and $S$ = 1.32 for 7272 reflections with $I > 2\sigma(I)$, and $R(F)$ = 0.1155, $wR(F^2)$ = 0.1681, and $S$ = 1.07 for 13 775 unique reflections and 649 parameters. The maximum $\Delta/\sigma$ in the final cycle of least squares was less than 0.001, and the residual peaks on the final difference Fourier map ranged from −0.298 to 0.443 eÅ$^{-3}$. Scattering factors were taken from the *International Tables for Crystallography*, Volume C.[91,92]

**Titration of Fe(OH)TMP with Fluorenone Oxime.** To 0.8 mL of a benzene-$d_6$ solution of Fe(OH)TMP (2.4 mM) was added small aliquots of solid fluorenone oxime. A $^1$H NMR spectrum of the sample was taken after thorough mixing. The spectrum showed that the resonance signals of Fe(OH)TMP changed to those of **2** within minutes, and the amount of **2** generated was proportional to that of the oxime added. The conversion was complete upon the addition of 1 equiv of fluorenone oxime. Further addition of fluorenone oxime led to the emergence of the signals of free fluorenone oxime without interfering signals of any other species.

**Oxidation of Fe(oximate)TMP (2) at High $O_2$ Pressures.** A high-pressure reaction vessel was made from stainless steel by our departmental machine workshop. The reactor contains a 30 mL Teflon liner, and the high-pressure seal was achieved by pressing an O-ring between the stainless steel screw-cap and the Teflon liner. The pressure gauge on top of the reactor monitoring the presure in the liner and two separate gas inlet and outlet values allow the control of the gas content inside the Teflon liner.

A 2 mL silanized glass vial containing a 0.8 mL benzene-$d_6$ solution of 0.75 mM **2** was enclosed in the high-pressure reactor. The reaction

(88) *COLLECT Data Collection Software.* Nonius B. V. Rontgenweg 1 P.O. Box 811, 2600 AV, Delft, The Netherlands, 1998.

(89) Otwinowski, Z.; Minor, W. *Methods Enzymol.* **1997**, *276*, 307.

(90) Sheldrick, G. M. *SHELXTL Version 5.04.*; Siemens Analytical X-ray Instruments: Madison, WI, 1996.

(91) Maslen, E. N.; Fox, A. G.; O'Keefe, M. A. In *International Tables for Crystallography: Mathematical, Physical and Chemical Tables*; Wilson, A. J. C., Ed: Kluwer: Dordrecht, The Netherlands, 1992; Vol. C, p 476.

(92) Creagh, D. C.; McAuley, W. J. In *International Tables for Crystallography: Mathematical, Physical and Chemical Tables*; Wilson, A. J. C., Ed: Kluwer: Dordrecht, The Netherlands, 1992; Vol. C, p 206.

(93) Van der Sluis, P.; Spek, A. L. *Acta Crystallogr., A* **1990**, *46*, 194.

(94) Spek, A. L. *Acta Crystallogr., A* **1990**, *46*, C34.

mixture was stirred with a magnetic stirrer. The oxidation was started by introducing various pressures of $O_2$ (>99.8% purity, from BOC gas) into the reactor. After a certain length of reaction time, the reactions was stopped by venting the $O_2$ from the reactor, and the content in the vial was analyzed with $^1$H NMR spectroscopy. The reactions were conducted at 100, 200, 330, and 500 psi $O_2$.

**Oxidation of Fe(oximate)TMP (2) under $^{18}O_2$.** The $^{18}O_2$ (98% enriched, from Cambridge Isotopes Laboratories) experiment was conducted on a high-vacuum Schlenk line. Into a 80 mL silanized flask was added a 50 mL benzene solution of 20 $\mu$M **2**, which was deaeriated (via three freeze−pump−thaw cycles) to remove the dissolved gas. Then 250 mL of 1 atm $^{18}O_2$ was introduced into the flask and condensed with liquid $N_2$ cold bath. The flask was then sealed with a J-Young valve, and the solution was warmed to 25 °C and stirred in the dark. The final $O_2$ pressure in the reaction flask was measured with a pressure gauge to be 100 ± 5 psi. The reaction was stopped 4 days later by releasing the $O_2$ pressure, and the solvent was removed by evacuation. The solid product was dissolved in benzene-$d_6$ and analyzed with $^1$H NMR spectroscopy, which showed that all **2** was consumed. The NMR sample was reduced to dryness and then triturated with acetonitrile to remove the iron porphyrins. The fluorenone-containing solid residue was redissolved in $CH_2Cl_2$ and analyzed with GC−MS. The relative ion abundances of the fluorenone peak in the mass spectrum are as follows: *m*/*z* (relative intensity) 179 (0.0), 180 (30.5), 181 (5.9), 182 (100.0), 183 (15.2), 184 (1.0). For comparison, the mass spectrum of fluorenone generated in the $^{16}O_2$-effected oxidation of **2** showed the following ratios: 179 (0.4), 180 (100.0), 181 (13.8), 182 (0.8), 183 (0).

**Aerobic Oxidation of Fluorenone Oxime.** A 0.75 mM benzene-$d_6$ solution of fluorenone oxime was purged with and kept under 1 atm $O_2$ at 35 °C in the dark. The reaction mixture was analyzed by $^1$H NMR spectroscopy every 24 h for 2 weeks. The $^1$H NMR spectrum showed that fluorenone oxime was oxidized in 1 week to **1**, which gradually decomposed to a one-to-one ratio of fluorenone and 9,9-dinitrofluorene over another week.

**Reaction of Fe(oximate)TMP (2) and $CO_{(g)}$. (a) UV−Visible Experiment.** A 3 mL benzene solution of 7 $\mu$M **2** in a cuvette was purged with $CO_{(g)}$ for 5 min at 10 °C. The cuvette was equipped with an enlarged headspace (∼80 mL). The cuvette was sealed with a J-Young valve under 1 atm $CO_{(g)}$, and the sample was warmed to room temperature and analyzed with UV−visible spectroscopy immediately. The UV−visible spectrum of the mixture showed that the absorbance due to **2** was gradually converted to $\lambda_{max}$ at 410, 426 (sh), 502, and 510 nm, which were the same as those of Fe(CO)TMP/Fe(CO)$_2$TMP.

**(b) Kinetic Experiment for the Eyring Plot.** To avoid the interference of irradiation on the product ratio, the same reaction mixture described above was prepared in the dark. A modified Cary 2390 UV−visible spectrophotometer was used to monitor the progress of the reaction. Located between the light source and the sample cuvette in the spectrophotometry was an electrical shutter controlled with a manual switch. The shutter was open for 2 s at each measurement. The absorbance at 426 nm was measured every 3 min for the first 2 h and then once each half hour for 12 h. The experiment was conducted at 30, 40, and 50 °C.

**Aerobic Oxidation of Fe(NO)TMP.** A benzene-$d_6$ solution of 1 mM Fe(NO)TMP was sealed in an NMR tube under 14.7 psi $O_2$. The sample was kept in a 50 °C bath in the dark and analyzed with $^1$H NMR spectroscopy every 12 h. The $^1$H NMR spectrum showed that Fe(NO)TMP converted gradually via a 5-coordinate high-spin Fe(III)-TMP species to Fe($NO_3$)TMP ($t_{1/2} \approx 2$ day). The new Fe(III)TMP species gave resonance signals at $\delta$ 76 (8H, pyrrole H), 13.3 and 14.6 (8H, *m*-phenyl H), 3.8 (12H, *p*-methyl H), and 2−6 (24H, *o*-methyl H).[34] The same reaction conducted at 25 °C showed that Fe(NO)TMP was oxidized much slower ($t_{1/2} \approx 1$ week). When the reaction was conducted under 500 psi $O_2$ at 25 °C, the half-life of Fe(NO)TMP was shortened to 10 h.

**Preparation and Characterization of the Putative Fe(ONO)TMP Complex.** Two milliliters (100-fold excess) of $NO_{(g)}$ was introduced to a 2.5 mM toluene-$d_8$ solution of Fe(OH)TMP in an air-free NMR tube. The solution immediately changed from dark green to bright red upon contact with NO. After the NMR tube was sealed with a J-Young valve, the sample was analyzed with $^1$H NMR spectroscopy. In addition to Fe(NO)TMP, the $^1$H NMR spectrum showed that a diamagnetic Fe(II)TMP species was the only other product, with resonance signals at $\delta$ 1.75 (s, 12H), 2.0 (s, 12H), 2.5 (s, 12H), and 8.8 (s, 8H, pyrrole-H).[34]

This diamagnetic Fe(II)TMP species was unstable and tended to lose one ligand upon extensive evacuation. After evacuating the sample to <1 $\mu$mHg vacuum for 2 days, the $^1$H NMR spectrum of the sample in anaerobic benzene-$d_6$ revealed that the diamagnetic Fe(II)P species had changed to a new 5-coordinate high-spin Fe(III)TMP species with resonance signals at $\delta$ 76 (8H, pyrrole H), 13.3 and 14.6 (8H, *m*-phenyl H), 3.8 (12H, *p*-methyl H), and 2−6 (24H, *o*-methyl H). By contrast, Fe(NO)TMP remained unchanged upon extensive evacuation. Upon exposing the sample to $O_2$ for a few days, the $^1$H NMR spectrum showed that the new Fe(III)TMP species and Fe(NO)TMP were both converted to Fe($NO_3$)TMP. This new 5-coordinate high-spin Fe(III)TMP species was tentatively assigned as Fe(ONO)TMP.

**Aerobic Oxidation of Fe(NO)TMP.** A benzene-$d_6$ solution of 1 mM Fe(NO)TMP was sealed in an NMR tube under 14.7 psi $O_2$. The sample was kept in a 50 °C bath in the dark and analyzed with $^1$H NMR spectroscopy every 12 h. The $^1$H NMR spectrum showed that Fe(NO)TMP converted gradually via the putative Fe(ONO)TMP species to Fe($NO_3$)TMP ($t_{1/2} \approx 2$ day). The same reaction conducted at 25 °C showed that Fe(NO)TMP was oxidized more slowly ($t_{1/2} \approx 1$ week). When the reaction was conducted under 500 psi $O_2$ at 25 °C, the half-life of Fe(NO)TMP was shortened to 10 h.

**Acknowledgment.** Financial support of this research from the National Institutes of Health (Grant GM36928) is gratefully acknowledged.

JA992373+